Hindawi
Advances in Civil Engineering
Volume 2019, Article ID 2647387, 15 pages
https://doi.org/10.1155/2019/2647387

Research Article

Seismic Response of Steel SMFs Subjected to Vertical Components of Far- and Near-Field Earthquakes with Forward Directivity Effects

Shahrokh Shahbazi,[1] Iman Mansouri,[2] Jong Wan Hu ,[3,4] Noura Sam Daliri,[5] and Armin Karami[6]

[1]*TAAT Investment Group, Tehran 18717-13553, Iran*
[2]*Department of Civil Engineering, Birjand University of Technology, P.O. Box 97175-569, Birjand, Iran*
[3]*Department of Civil and Environmental Engineering, Incheon National University, Incheon 22012, Republic of Korea*
[4]*Incheon Disaster Prevention Research Center, Incheon National University, Incheon 22012, Republic of Korea*
[5]*Department of Civil Engineering, University of Science and Culture, Tehran, Iran*
[6]*Department of Civil, Environmental and Land Management Engineering, Politecnico di Milano, Milan 20133, Italy*

Correspondence should be addressed to Jong Wan Hu; jongp24@incheon.ac.kr

Received 21 November 2018; Revised 25 February 2019; Accepted 10 March 2019; Published 3 April 2019

Academic Editor: Lyan-Ywan Lu

In the near-field earthquake, forward directivity effects cause long-period pulse with a short effective time and a large domain in the velocity time history. This issue increases the ductility needs of structures, and in recent decades, the destructive effects of these kinds of records have been evaluated in comparison with far-field earthquakes. This brings about the necessity to compare a structure's behavior subjected to vertical components of near-field (NF) earthquakes, including forward directivity effects vs. the effects of vertical components of far-field (FF) earthquakes. The present study investigated 3-, 5-, 8-, and 20-story steel moment frames with special ductility (SMF) through which modeling effects of panel zone have been applied, subjected to vertical component of near-field (NF) earthquakes with forward directivity and the vertical component of far-field earthquakes. By investigating the results, it can be clearly seen that the average values of the maximum displacement, shear force of the stories, and the velocity of each story under the impact of the near-field earthquake are greater than the amount of that under the effect of a far-field earthquake. However, this comparison is not valid for the amount of acceleration, axial force, and moments in the columns of the structures accurately.

1. Introduction

Near-fault (NF) ground motions are specified by long-period velocity and displacement pulses [1] and high values of the ratio between the peak of vertical and horizontal ground accelerations [2]. In near-fault earthquakes, the fault geometry position related to the considered place is significant besides the rupture mechanism and kind of faulting. The amplitude of this pulse depends on the directivity of rupture distribution to the site. Since the rupture diffusion velocity is almost the same as the velocity of shear wave diffusion, if the fault rupture propagates to the considered place, the waves in a short-term period will reach to the place resulted in a pulse with high amplitude and short period that is called forward-effect directivity [3, 4].

Over the past thirty years, there have been leading developments in the way that characteristics of vertical ground motion are interpreted and quantified [5–9]. In comparison with other studies, these researches have determined that vertical response spectra are most susceptible to spectral period and source-to-site distance. Additionally, the vertical-to-horizontal (V/H) response spectral ratios are higher on soil than on rock, and at shorter periods than at longer periods, in general [10].

In engineering design, the vertical-to-horizontal acceleration (V/H) ratios of peak ground acceleration are usually recommended as 2/3. Moreover, the shape of the vertical response spectrum is similar to that of the horizontal response spectrum. During the recent years, it was understood that the areas near the epicenter and faults exert a strong vertical ground motion. The vertical-to-horizontal V/H response spectral ratios are greater than 2/3. The ratios for long periods were smaller than the value of that for short periods. In the past studies, it has been found that the V/H response spectral ratios are potently related to the period and site-to-source distance during the 1994 Northridge earthquake [11].

In the seismic design of critical structures such as nuclear power plants and dams, vertical ground motions are frequently considered. However, some researches over the previous ten years recommend that the vertical ground motion component can have a great impact on the seismic response of common highway bridges especially for the sites placed in almost 15 km of major faults, as well [12–14].

Although, in recent years, nonlinear dynamic analysis has become standard practice to figure out the seismic performance of structures, applying the direct analysis to evaluate the critical demands is computationally expensive and difficult. As a result, the main goal of the present research is to perform extensive nonlinear dynamic analyses and obtain all important demands of structures for comparing the results of near-field and far-field ground motions.

In particular, the seismic response of steel moment frame with special ductility is investigated under the effect of panel zone modeling subjected to vertical components of near-field earthquakes with the forward directivity effect and vertical components of far-field earthquakes. To this end, velocity, vertical acceleration, vertical displacement, column axial force, moment column, and the shear force of the stories under the impact of far- and near-field earthquakes have been compared in 3-, 5-, 8-, and 20-story structures.

In previous studies, the comparison of near-field and far-field earthquakes has been mentioned repetitively. However, near-field earthquakes are divided into two subdivisions: forward directivity and filling step. This research is the first to study the effect of the vertical component of near-field and far-field earthquake with forward directivity on the behavior of steel moment frames with special ductility. In order to obtain better results of this comparison, some of the major elements for the engineers and designers, e.g., axial force in the columns, generated a moment in the columns, maximum drift, and shear force, have been applied.

2. Characteristics of Modeled Buildings

In the present paper, 3-, 5-, 8-, and 20-story buildings were selected for the analysis. All modeled structures are shown in Figure 1. Also, the 20-story building is represented from reference [15]. According to the classification of the HAZUS-MH MR5 [16] instruction, 3-, 5-, 8-, and 20-story buildings are categorized as low-, middle-, and high-rise buildings.

The lateral resisting systems are the special moment resisting frame in X and Y directions. They were used in order to examine the seismic behavior of four models constructed in very high-risk zones on soil type III. ETABS software and Iranian national building code [17] were used for the seismic design of these four models.

According to the European standard profiles, different types of profiles were considered for beams and columns. As a result, profile we were used for the beams, and the box-shaped section was considered for columns (Table 1).

Different assumptions were made in the present study. In all stories, dead and live loads were 650 kg/m^2 and 200 kg/m^2, respectively. However, different loads were applied for roofs, at 540 kg/m^2 and 150 kg/m^2, respectively. The columns are assumed to be axially flexible. Thus, the beams should be simulated as flexible members in all directions [18]. In a real structure, the vertical flexibility (bending) of very stiff beams is larger than the axial flexibility of the columns. Elastic elements were considered for all beams and columns in OpenSees, a software application employed for modeling these structures. Bilin Material was used to describe the behavioral properties of the elements. In addition, the Krawinkler Panel Zone Model [19] was used (Figure 2).

The panel zone deforms primarily in shear due to the opposing moments in the columns and beams. The panel zone was explicitly modeled using the method of Gupta and Krawinkler [20] as a rectangle composed of eight very stiff elastic beam-column elements with one rotational spring to represent shear distortions in the panel zone [21] (Figure 2).

The Bilin Material imitates the Modified Ibarra-Medina-Krawinkler Deterioration Model with a bilinear hysteretic response. Figure 3 shows the parameters of Bilin Material. The relationships between variables were developed following Lignos and Krawinkler [22].

The fundamental horizontal periods of 3-, 5-, 8-, and 20-story buildings were 0.48, 0.91, 0.78, and 3.57 seconds, respectively. Moreover, the fundamental vertical periods of 3-, 5-, 8-, and 20-story buildings were 0.065, 0.11, 0.09, and 0.36 seconds, respectively.

To represent the structure's nonlinear behavior, the studied structures were modeled with elastic beam-column elements connected by rotational springs. Based on the Modified Ibarra Krawinkler Deterioration Model, the springs follow a bilinear hysteretic response.

The plastic hinge was modeled by a rotational spring placed in the middle of the reduced beam sections (RBS). An elastic beam-column element was used to connect the spring and the panel zone.

Since an elastic element as a model of a frame member was connected in series with rotational springs at either end, the stiffness of these components had to be modified in order that the equivalent stiffness of this assembly was equivalent to the stiffness of the actual frame member [23].

3. Near-Field Earthquakes

Near-field ground motions are more complex than the far-field records, and this difference can change the response

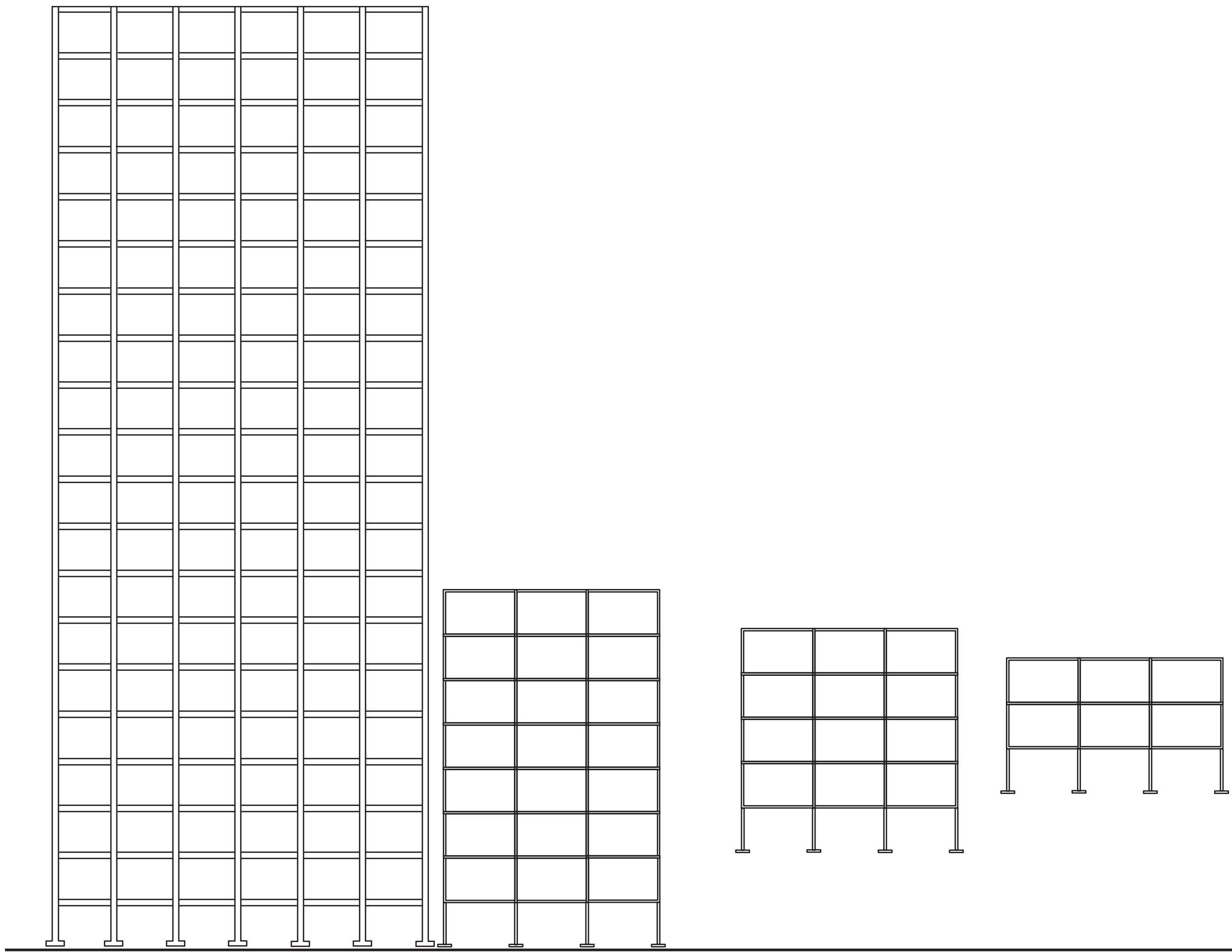

Figure 1: Topology of 20-, 8-, 5-, and 3-story buildings.

characteristics of the structure significantly. The main characteristics of near-field ground motions are as follows: (1) permanent displacement (fling) effect induced by the permanent tectonic offset of a rupturing fault; (2) severe impulsive velocity effect observed in the velocity time histories of various strong-motion earthquakes (e.g., 2015 Nepal earthquake); and (3) hanging-wall by which earthquakes at sites placed on the hanging wall of a dip-slip fault are larger than at sites placed on the footwall at the same distance [24].

In earthquakes occurring near the fault, diverse key factors, including geometry position, failure mechanism, and faulting, appear to be important. As in most cases with a high period describing a kind of excitation like a strike, ground velocity can result in pulse [25]. In addition, one of the features of near-field earthquake records including forward directivity is the existence of long-period pulses in their velocity time history. These pulses can be observed in the velocity time history of the vertical and horizontal components of these records (Figure 4).

4. Selection of Ground Motions

In the evaluation of structures in time history analyses, various factors seem to play a major role. The selection of ground motions has been made so that they all represent the $Mw = 6.5$ template scenario as the result of the risk segmentation in Iran's with very high seismic zones. Furthermore, as the conditions of a site have a significant effect on the characteristics and frequency content of the strong ground motion records, the ground motions were selected to ensure that the average of the spectrum resultant closely matches the design spectrum at all periods (Figures 5 and 6). Based on this, 15 earthquake records for both near- and far-field subjected to forward directivity have been considered for the evaluation of nonlinear time-history. Near- and far-field earthquakes which were calculated on type 3 soil have been recorded in the maximum from 10 to 100 km away from the fault, respectively. The magnitudes of near- and far-field earthquakes ranged from 6.53 to 6.93 moment magnitude scale and 6.4 to 7.5 moment magnitude scale, respectively. Tables 2 and 3 demonstrate the seismographs and their related characteristics.

5. Evaluation of Seismic Response of Structures

The ground motions were scaled so that the average value of their square root of the sum of the squares (SRSS)

Table 1: Sections of 3-, 5-, and 8-story structures.

	No.	Column	Beam
3-story	1	Tube 200 × 200 × 20	IPE 300
	2	Tube 200 × 200 × 20	IPE 300
	3	Tube 200 × 200 × 20	IPE 270
	4	Tube 280 × 280 × 20	IPE 400
	5	Tube 280 × 280 × 20	IPE 300
	6	Tube 280 × 280 × 20	IPE 270
5-story	1	Tube 240 × 240 × 20	IPE 330
	2	Tube 240 × 240 × 20	IPE 360
	3	Tube 180 × 180 × 20	IPE 240
	4	Tube 300 × 300 × 20	IPE 330
	5	Tube 300 × 300 × 20	IPE 360
	6	Tube 240 × 240 × 20	IPE 240
8-story	1	Tube 340 × 340 × 20	IPE 450
	2	Tube 340 × 340 × 20	IPE 450
	3	Tube 280 × 280 × 20	IPE 450
	4	Tube 200 × 200 × 20	IPE 360
	5	Tube 400 × 400 × 20	IPE 450
	6	Tube 400 × 400 × 20	IPE 450
	7	Tube 340 × 340 × 20	IPE 450
	8	Tube 280 × 280 × 20	IPE 360

The below syntax is used for the position of columns and beams in the result of analysis (Table 8). C^*_{ij} is the code for location of columns results. i = number of stories. B^*_{ik} is the code for location of beams results. j = number of columns from the left of structures. k = number of spans from the left of structures.

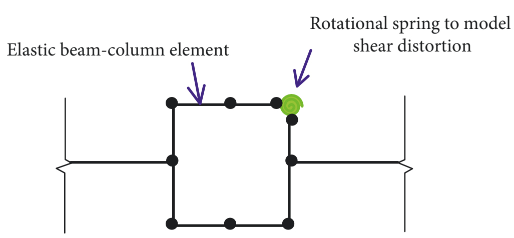

Figure 2: Schematic representation of a typical panel zone [19].

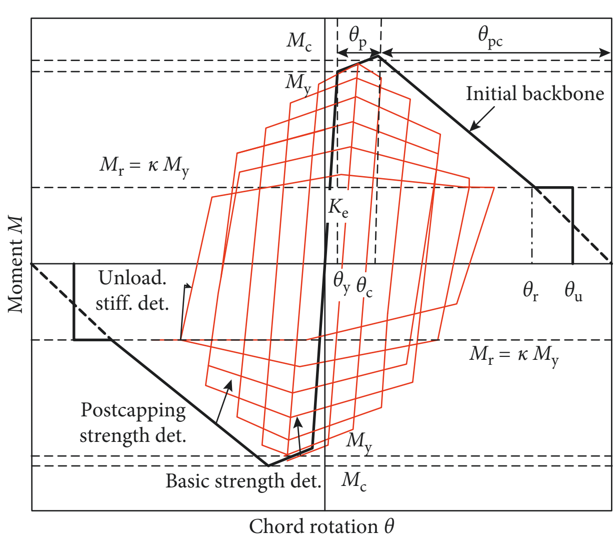

Figure 3: The Modified Ibarra-Medina-Krawinkler Deterioration Model [22].

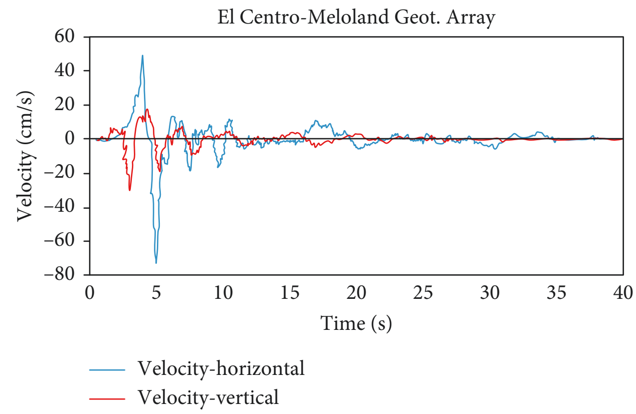

Figure 4: Velocity-time history of vertical and horizontal components of near-field earthquake with the effect of forward directivity.

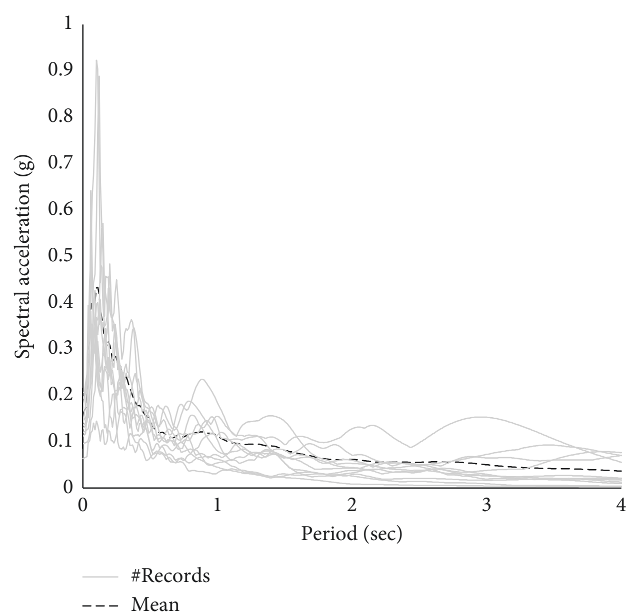

Figure 5: Elastic response spectral acceleration for far-field records.

spectra did not fall below 1.4 times the Standard Design-Spectra for periods of $0.2T$ second to $1.5T$ seconds, where T is the fundamental period of vibration [17]. Figure 7 shows the elastic response spectra for 5% damping of these selected near-field ground motions, as well as the process of scaling for the 8-story building. In OpenSees, three types of stiffness matrix can be considered for the Rayleigh damping command: current stiffness matrix, initial stiffness matrix, and committed stiffness matrix. In the inelastic analysis, the “committed stiffness matrix” should be employed.

Totally, in the present research, 120 nonlinear time history analyses were performed according to the 30 selected records and the number of considered buildings.

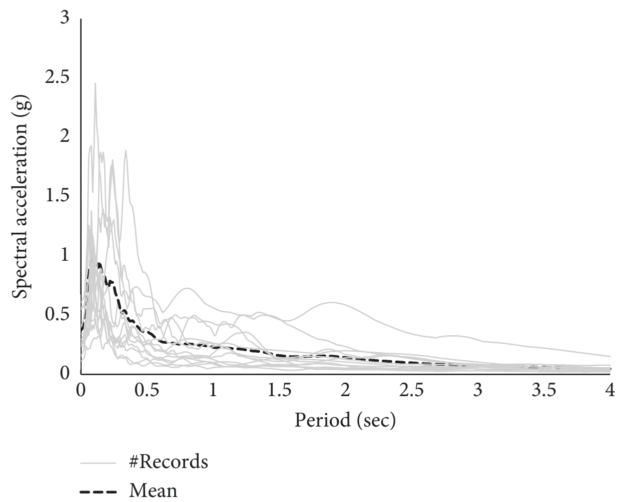

Figure 6: Elastic response spectral acceleration for near-field records.

Table 2: Near-field records.

#Records	Event name	Year	Station	Mw	Vertical PGA (g)	PGA (g)	*R* (km)
#Record1	Erzican	1992	Erzican	6.69	0.234	0.49	2
#Record2	Imperial Valley	1979	EC country	6.53	0.244	0.23	7.31
#Record3	Imperial Valley	1979	"El Centro-Meloland Geot. Array"	6.53	0.248	0.32	0.07
#Record4	Kobe	1995	KJMA	6.9	0.338	0.83	0.94
#Record5	Kobe	1995	"Port Island (0 m)"	6.9	0.566	0.35	3.31
#Record6	Kobe	1995	Takatori	6.9	0.284	0.67	1.46
#Record7	Northridge-01	1994	Newhall-Fire Sta	6.69	0.548	0.59	3.16
#Record8	"Imperial Valley-06"	1979	"Brawley Airport"	6.53	0.1528	0.22	8.54
#Records9	Loma Prieta	1989	Saratoga-W Valley Coll	6.93	0.3957	0.33	8.48
#Records10	Northridge-01	1994	Rinaldi Receiving Sta	6.69	0.958	0.87	0
#Records11	Northridge-01	1994	Sylmar-Converter Sta	6.69	0.605	0.92	0
#Records12	"Imperial Valley-06"	1979	"El Centro Array #10"	6.5	0.109	0.14	6.2
#Records13	"Imperial Valley-06"	1979	"Holtville Post Office"	6.5	0.256	0.26	7.7
#Records14	"Loma Prieta"	1989	"Gilroy Array #2"	6.93	0.295	0.32	12.7
#Records15	"Loma Prieta"	1989	"Gilroy Array #3"	6.93	0.341	0.37	14.4

PGA: peak ground acceleration.

Table 3: Far-field records.

#Records	Event name	Year	Station	Vertical PGA (g)	PGA (g)	Mw	*R* (km)
#Record1	Imperial Valley-06	1979	Calexico, Fire Station	0.193	0.27	6.5	10.45
#Record2	Kocaeli_ Turkey	1999	Duzce	0.206	0.36	7.5	98.2
#Record3	Landers	1992	Palm Springs, Airport	0.111	0.075	7.2	36.15
#Record4	Landers	1992	Yermo Fire station	0.1358	0.24	7.3	86
#Record5	Loma Prieta	1989	Coyote Lake Dam, downstream	0.095	0.18	7.1	20.8
#Record6	San Frenando	1971	LA-Hollywood stor	0.164	0.22	6.6	39.5
#Record7	Big Bear	1992	Desert Hot Spr	0.119	0.22	6.4	39.5
#Record8	"Imperial Valley-06"	1979	"Delta"	0.142	0.35	6.53	33.7
#Records9	"Imperial Valley-06"	1979	"El Centro Array #11"	0.143	0.38	6.5	29.4
#Records10	"Kobe_Japan"	1995	"Shin-Osaka"	0.063	0.23	6.9	46
#Records11	"Superstition Hills-02"	1987	"El Centro Imp. Co. Cent"	0.127	0.35	6.5	35.8
#Records12	Loma Prieta	1989	Gilroy Array #3	0.3416	0.56	6.9	31.4
#Records13	Chi chi	1999	Chy101	0.165	0.44	7.6	32
#Records14	Duzce	1999	Bolu	0.2	0.82	7.1	41.3
#Records15	Northridge	1994	Hollywood—Willoughby Ave	0.151	0.25	6.69	23.07

In this study, the total acceleration response has been evaluated. By comparing the peak floor amplifications under the influence of near-field (NF) and far-field (FF) earthquakes, it was determined that, in the NF shocks with forward directivity in the 3-story building, peak floor amplifications was 0.106 g, under the #Record11 record; in the

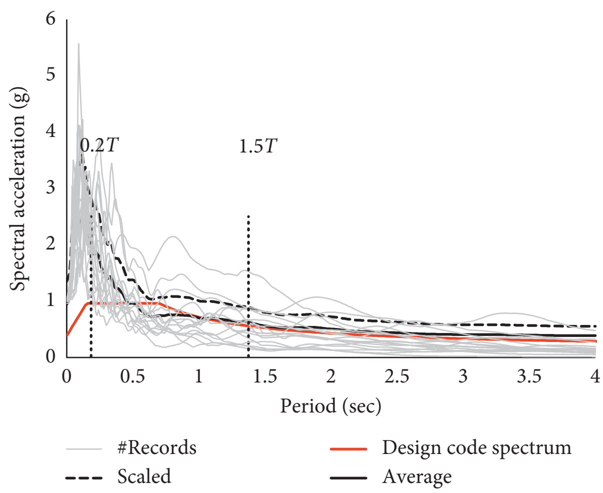

Figure 7: Process of scaling for the 8-story building.

5-story building, it was 0.067 g, which is the location on the fifth floor under the #Record10 record; for the 8-story building, it was 0.506 g, which is located on the seventh floor under the #Record11 record; finally, in the 20-story building, it was 1.818, which is located on the third floor under the #Record10. On the other hand, in each of the four structures under the influence of FF earthquakes, the peak floor amplification values of the floors amounted to 0.067 g, 0.068 g, 0.669 g, and 0.557 g. For a more accurate evaluation, a comparison of the average value of the peak floor amplifications of stories was made (Table 4).

By investigating the maximum roof displacement subjected to far- and near-field earthquakes, we found that near-field earthquakes including forward directivity in the 3-story building resulted in the maximum displacement in the roof (0.74 mm). In the 5-story building, near-field earthquakes caused a 0.80 mm displacement, which is 1.73 times greater than the displacement subjected to the vertical component of far-field earthquakes. This parameter can also be seen in 8-story building with the corresponding values of 0.96 mm for near-field and 0.62 mm for far-field earthquakes. At the end, the maximum roof displacement in the 20-story building with the corresponding values of 0.817 mm for near-field and 0.556 mm for far-field earthquakes.

Table 4 shows a comparison of the maximum roof displacements by the influence of far- and near-field earthquakes. Figure 8 shows the graphs related to the maximum displacement of the stories under the effect of near- and far-field earthquakes. Furthermore, for a more accurate investigation, the results of a comparison of the average roof displacements are given in Table 4.

From the results of the analysis shown in Table 5, the maximum axial forces in the 3-story structure subjected to near-field earthquakes were by 13% greater than those same forces subjected to far-field earthquakes. In the 5-story structure, the axial forces in the columns in both records of far- and near-field earthquakes were almost equal. In addition, the maximum axial force produced in the 8-story structure under the effect of near-field earthquakes was by 22% lower than that subjected to far-field earthquakes. Furthermore, in the 20-story structure, the maximum axial force subjected to near-field earthquakes was by 26% higher than that subjected to far-field earthquakes.

Table 4: Comparison of the average value of the peak floor amplification of stories and roof displacement subjected to near- and far-field earthquakes.

	Story	FF	NF	NF/FF
Acceleration (g)	3	0.029	0.038	1.310
	5	0.026	0.025	0.961
	8	0.189	0.198	1.047
	20	0.304	0.705	2.319
Displacement (mm)	3	0.23	0.33	1.43
	5	0.25	0.35	1.40
	8	0.38	0.48	1.26
	20	0.26	0.35	1.35

As can be seen from the results shown in Table 6, the ratio of the maximum moment subjected to vertical component of near-field earthquakes to the maximum moment generated under the effect of vertical component of far-field earthquakes in all four structures (3-, 5-, 8-, and 20-story) was 1.07, 0.96, 0.77, and 1.08, respectively.

From the results shown in Figure 9 and Table 7, it can be clearly observed that the maximum shear force generated in 3- and 8-story buildings subjected to the vertical component of near-field earthquakes was by 6% and 24% lower than far-field earthquakes, respectively, and in 5- and 20-story buildings subjected to the vertical component of near-field earthquakes was by 7% and 31% higher than far-field earthquakes, respectively. In the end, the moment of beams has investigated, and the result is shown in Table 8.

Finally, the results of this paper are summarized based on the comparison methodology in references [26, 27]. Tables 9 and 10 show that the peak vertical floor acceleration (named as *PFA*v) may exceed the peak vertical ground acceleration (named as *PGA*v). The results demonstrate that the ratio of *PFA*v/*PGA*v in 3-, 5-, 8-, and 20-story buildings under near-field records is 1.79, 1.27, 3.17, and 24.68, respectively. Moreover, this ratio for those buildings subjected to far-field records is 3.30, 4.69, 25.88, and 25.26.

6. Conclusions

The present study has evaluated the seismic behavior of special steel moment frames of 3-, 5-, 8-, and 20-story buildings subjected to the vertical components of far- and near-field earthquakes. According to the classification of the HAZUS-MH MR5 [16] instruction, 3-, 5-, 8-, and 20-story buildings are categorized as low-, middle-, and high-rise buildings. From the results of the nonlinear time history analysis for the models studied, the following conclusions can be drawn:

(i) One of the major elements in evaluating the seismic behavior of structures is known as displacement. This study shows that the amount of forced displacement to the structure under the effect of the

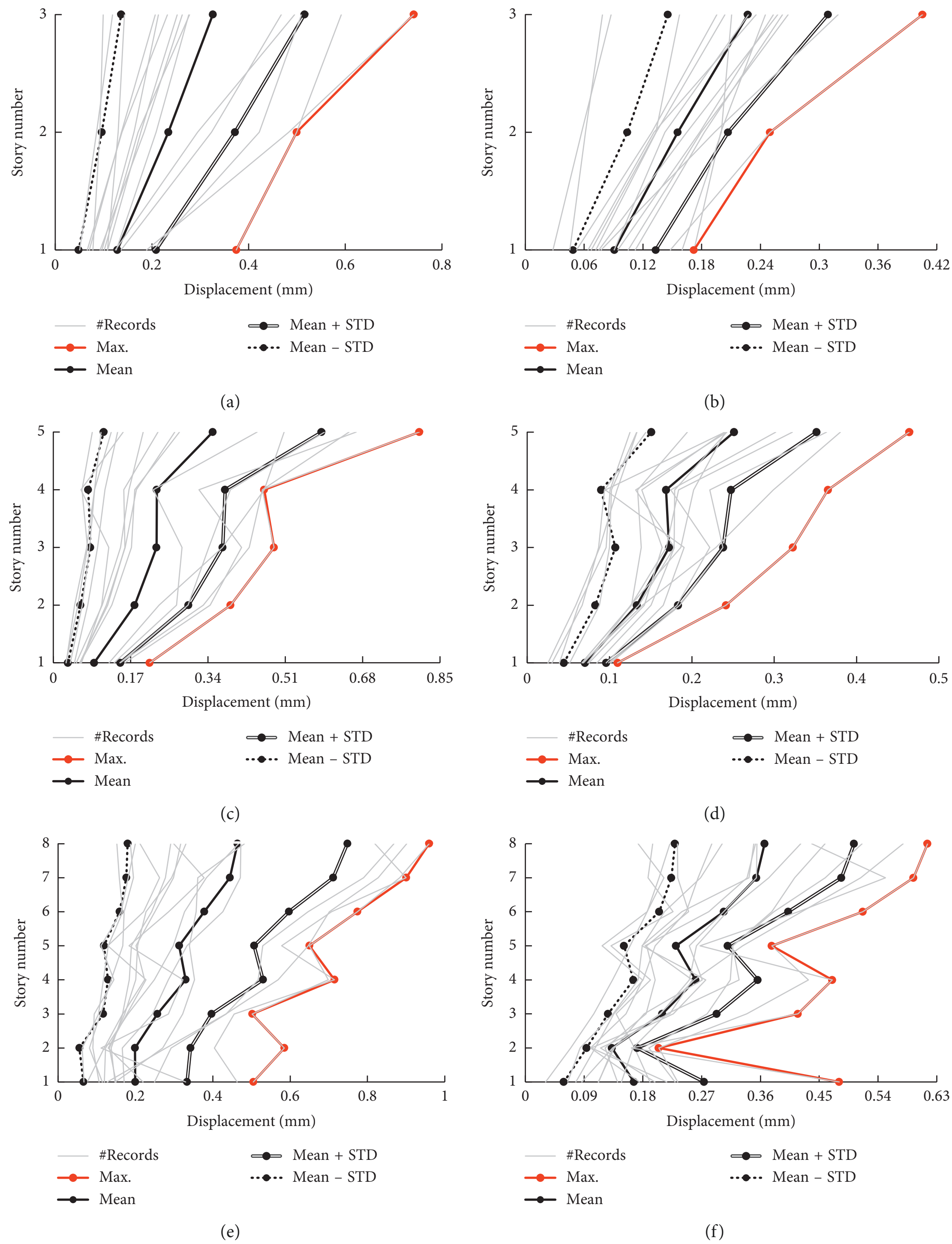

Figure 8: Continued.

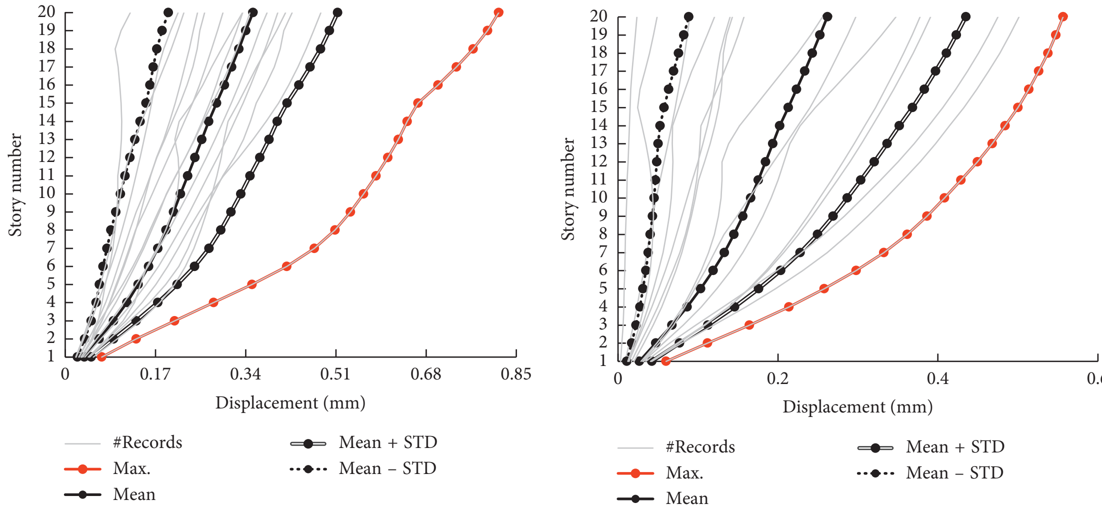

(g) (h)

Figure 8: Maximum displacement in 3-, 5-, 8-, and 20-story building subjected to near- (a, c, e, g) and far-field (b, d, f, h) earthquakes.

Table 5: Comparison of the maximum axial force of columns in 3-, 5-, 8-, and 20-story buildings subjected to near- and far-field earthquakes.

	No. of stories	Field	Axial column force (kN)	No. of columns	Record	Near/far
3-story	1	Near	61.750	C14	#Records11	1.129
		Far	54.67	C11	#Record12	
	2	Near	42.224	C14	#Records11	1.031
		Far	40.92	C11	#Record12	
	3	Near	27.819	C14	#Records11	1.058
		Far	26.29	C11	#Record12	
5-story	1	Near	105.099	C14	#Records10	0.999
		Far	105.13	C14	#Record8	
	2	Near	96.120	C14	#Records10	0.991
		Far	96.95	C14	#Record8	
	3	Near	75.586	C14	#Records10	0.983
		Far	76.91	C14	#Record8	
	4	Near	54.298	C14	#Records10	0.984
		Far	55.20	C14	#Record8	
	5	Near	26.702	C14	#Records10	0.963
		Far	27.73	C14	#Record8	
8-story	1	Near	357.76	C14	#Records11	0.780
		Far	458.40	C14	#Record12	
	2	Near	337.45	C14	#Records11	0.775
		Far	435.56	C14	#Record12	
	3	Near	301.11	C14	#Records11	0.776
		Far	388.22	C14	#Record12	
	4	Near	261.27	C14	#Records11	0.778
		Far	335.63	C14	#Record12	
	5	Near	209.32	C14	#Records11	0.765
		Far	273.72	C14	#Record12	
	6	Near	165.23	C14	#Records11	0.763
		Far	216.69	C14	#Record12	
	7	Near	120.52	C14	#Records11	0.766
		Far	157.30	C14	#Record12	
	8	Near	71.40	C14	#Records15	0.742
		Far	96.28	C14	#Record12	

Table 5: Continued.

	No. of stories	Field	Axial column force (kN)	No. of columns	Record	Near/far
20-story	1	Near	14330.09	C14	#Records5	1.267
		Far	11312.26	C14	#Records13	
	2	Near	13563.66	C14	#Records5	1.283
		Far	10569.36	C14	#Records13	
	3	Near	12707.71	C14	#Records5	1.299
		Far	9780.81	C14	#Records13	
	4	Near	12707.71	C14	#Records5	1.402
		Far	9060.82	C14	#Records13	
	5	Near	11016.25	C14	#Records5	1.318
		Far	8356.13	C14	#Records13	
	6	Near	10155.81	C14	#Records5	1.324
		Far	7667.54	C14	#Records13	
	7	Near	9348.77	C14	#Records5	1.337
		Far	6988.96	C14	#Records13	
	8	Near	8556.42	C14	#Records5	1.354
		Far	6320.06	C14	#Records13	
	9	Near	7744.19	C14	#Records5	1.363
		Far	5680.05	C14	#Records13	
	10	Near	6917.78	C14	#Records5	1.365
		Far	5068.28	C14	#Records13	
	11	Near	6084.43	C14	#Records5	1.364
		Far	4461.07	C14	#Records13	
	12	Near	5227.68	C14	#Records5	1.313
		Far	3979.52	C14	#Records13	
	13	Near	4342.26	C14	#Records5	1.245
		Far	3488.41	C14	#Records13	
	14	Near	3558.95	C13	#Records4	1.203
		Far	2958.85	C14	#Records13	
	15	Near	2929.68	C13	#Records4	1.215
		Far	2410.56	C14	#Records13	
	16	Near	2303.32	C13	#Records4	1.230
		Far	1871.98	C14	#Records13	
	17	Near	1733.34	C13	#Records4	1.287
		Far	1347.13	C14	#Records13	
	18	Near	1181.83	C13	#Records4	1.348
		Far	876.72	C14	#Records13	
	19	Near	726.91	C13	#Records10	1.506
		Far	482.47	C14	#Records13	
	20	Near	312.53	C13	#Records10	1.766
		Far	176.97	C14	#Records13	

Table 6: Comparison of the maximum moment of columns in 3-, 5-, 8-, and 20-story buildings subjected to near- and far-field earthquakes.

	No. of story	Field	Moment (kN·M)	No. of columns	Record	Near/far
3-story	1	Near	34.817	C14	#Records11	1.513
		Far	23.00	C14	#Record12	
	2	Near	32.990	C14	#Records11	1.189
		Far	27.75	C14	#Record12	
	3	Near	47.073	C14	#Records11	1.069
		Far	44.05	C11	#Record12	
5-story	1	Near	16.428	C14	#Records10	1.043
		Far	15.74	C14	#Record12	
	2	Near	29.077	C14	#Records10	1.028
		Far	28.27	C14	#Record8	
	3	Near	30.849	C14	#Records10	0.986
		Far	31.29	C14	#Record8	
	4	Near	40.865	C14	#Records10	1.002
		Far	40.78	C14	#Record8	
	5	Near	45.906	C14	#Records10	0.958
		Far	47.93	C14	#Record8	

Table 6: Continued.

	No. of story	Field	Moment (kN·M)	No. of columns	Record	Near/far
8-story	1	Near	44.23	C12	#Records11	0.867
		Far	51.00	C12	#Record12	
	2	Near	55.70	C14	#Records11	0.780
		Far	71.42	C14	#Record12	
	3	Near	61.36	C14	#Records15	0.749
		Far	81.89	C14	#Record12	
	4	Near	78.98	C14	#Records11	0.836
		Far	94.48	C11	#Record12	
	5	Near	63.21	C14	#Records11	0.768
		Far	82.27	C14	#Record12	
	6	Near	63.77	C14	#Records11	0.755
		Far	84.51	C14	#Record12	
	7	Near	91.31	C14	#Records11	0.803
		Far	113.78	C14	#Record12	
	8	Near	111.68	C14	#Records11	0.773
		Far	144.50	C14	#Record12	
20-story	1	Near	3815.19	C13	#Records5	1.082
		Far	3526.56	C13	#Record13	
	2	Near	2140.55	C13	#Records5	1.183
		Far	1809.33	C13	#Record13	
	3	Near	1971.99	C13	#Records5	1.179
		Far	1672.12	C13	#Record13	
	4	Near	1862.47	C13	#Records5	1.109
		Far	1679.10	C13	#Record13	
	5	Near	2102.03	C13	#Records5	1.224
		Far	1717.44	C13	#Record13	
	6	Near	2107.63	C13	#Records5	1.379
		Far	1528.38	C13	#Record13	
	7	Near	1968.57	C13	#Records5	1.312
		Far	1499.84	C13	#Record13	
	8	Near	1735.88	C13	#Records5	1.190
		Far	1457.93	C13	#Record13	
	9	Near	1743.19	C13	#Records5	1.275
		Far	1367.14	C13	#Record13	
	10	Near	1788.47	C13	#Records5	1.418
		Far	1261.23	C13	#Record13	
	11	Near	2040.55	C13	#Records5	1.630
		Far	1251.65	C13	#Record13	
	12	Near	1884.31	C13	#Records5	1.605
		Far	1173.92	C13	#Record13	
	13	Near	2049.72	C13	#Records4	1.768
		Far	1159.12	C13	#Record12	
	14	Near	1819.52	C13	#Records4	1.585
		Far	1148.11	C13	#Record12	
	15	Near	1326.48	C13	#Records4	1.230
		Far	1078.67	C13	#Record12	
	16	Near	1282.13	C13	#Records4	1.197
		Far	1071.34	C13	#Record12	
	17	Near	1350.00	C13	#Records4	1.395
		Far	967.94	C13	#Record12	
	18	Near	1114.58	C13	#Records4	1.317
		Far	846.47	C13	#Record12	
	19	Near	1040.41	C13	#Records10	1.657
		Far	627.72	C13	#Record12	
	20	Near	730.75	C13	#Records10	1.817
		Far	402.19	C13	#Record12	

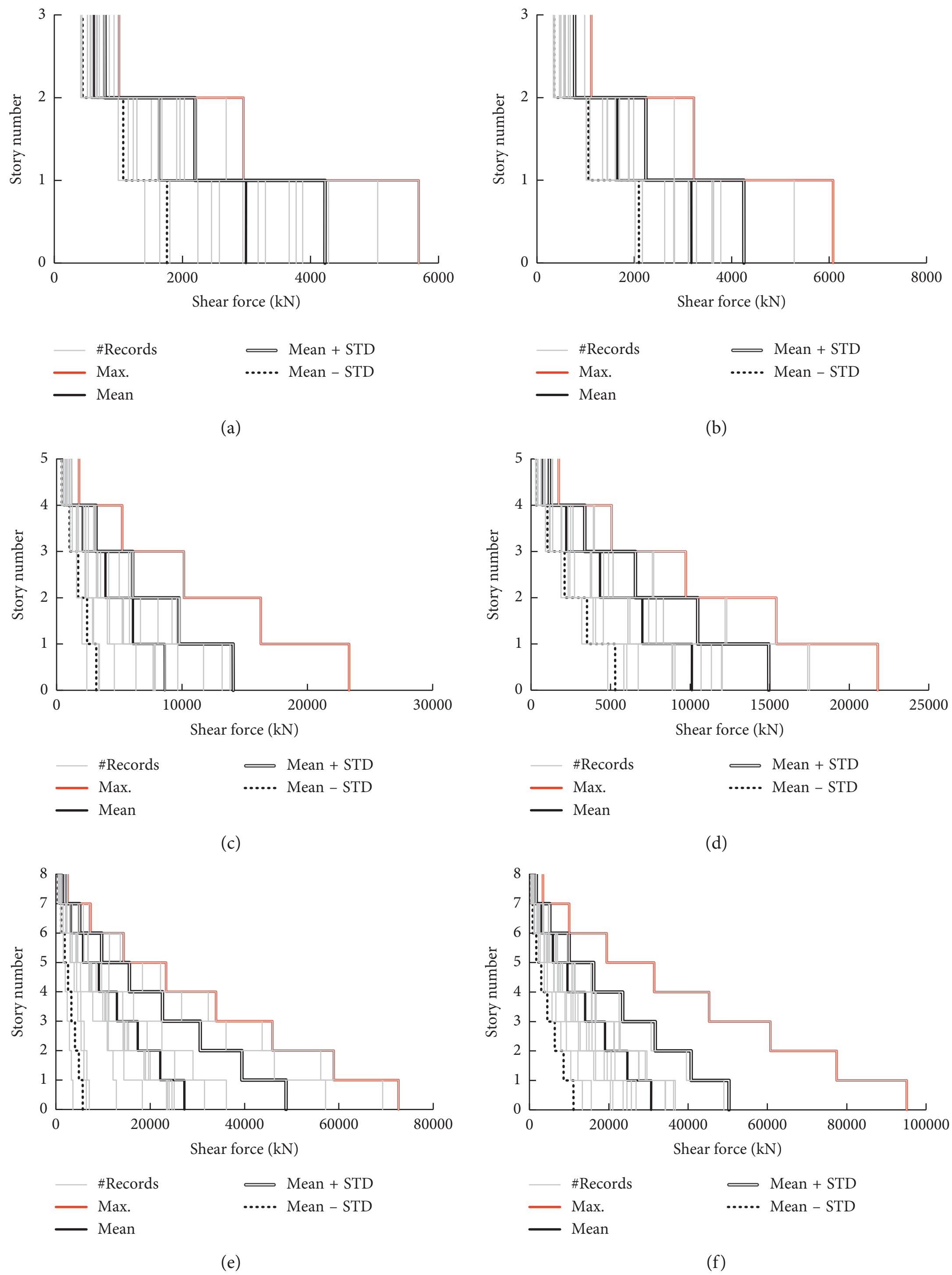

Figure 9: Continued.

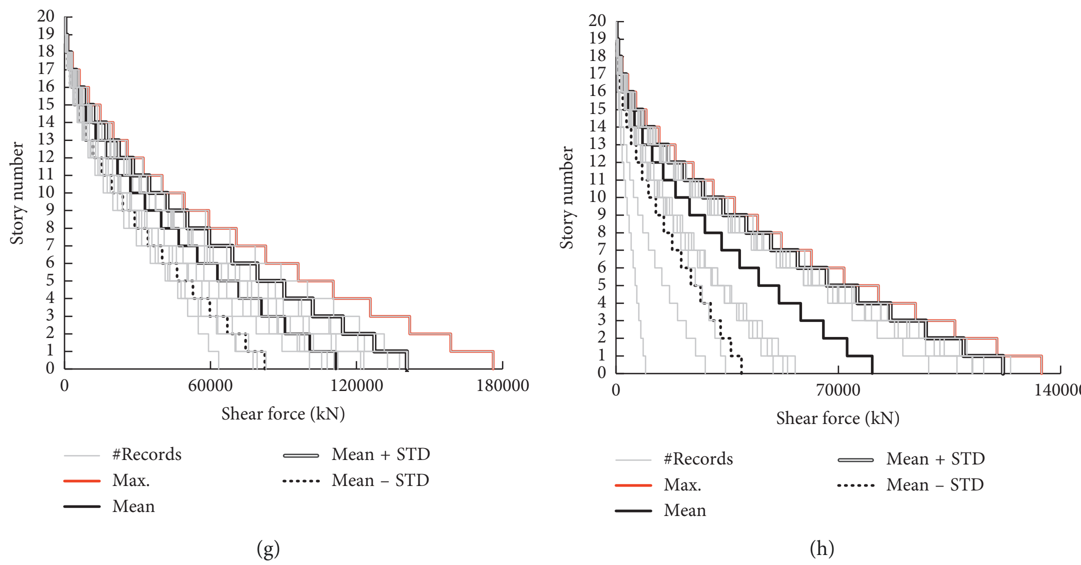

Figure 9: Shear force in 3-, 5-, 8-, and 20-story building subjected to near- (a, c, e, g) and far-field (b, d, f, h) earthquakes.

Table 7: Comparison of shear force in 3-, 5-, 8-, and 20-story buildings subjected to near- and far-field earthquakes.

	No. of story	Field	Shear force (kN)	Record	Near/far
3-story	1	Near	5690.151	#Record10	0.936
		Far	6079.894	#Record12	
	2	Near	2951.553	#Record10	0.916
		Far	3221.74	#Record12	
	3	Near	1010.715	#Record10	0.906
		Far	1115.286	#Record12	
5-story	1	Near	23330.8	#Record10	1.071
		Far	21790.943	#Record12	
	2	Near	16292.44	#Record10	1.057
		Far	15411.848	#Record12	
	3	Near	10167.194	#Record10	1.045
		Far	9730.468	#Record12	
	4	Near	5240.218	#Record10	1.034
		Far	5065.902	#Record12	
	5	Near	1786.496	#Record10	1.027
		Far	1738.721	#Record12	
8-story	1	Near	72626.839	#Record11	0.764
		Far	95117.604	#Record12	
	2	Near	58892.989	#Record11	0.760
		Far	77460.474	#Record12	
	3	Near	45891.719	#Record11	0.756
		Far	60714.82	#Record12	
	4	Near	33941.519	#Record11	0.749
		Far	45295.754	#Record12	
	5	Near	23344.349	#Record11	0.743
		Far	31422.154	#Record12	
	6	Near	14372.579	#Record11	0.737
		Far	19498.604	#Record12	
	7	Near	7332.913	#Record11	0.731
		Far	10026.224	#Record12	
	8	Near	2464.752	#Record11	0.726
		Far	3393.249	#Record12	

Table 7: Continued.

No. of story		Field	Shear force (kN)	Record	Near/far
20-story	1	Near	176111.944	#Records5	1.314
		Far	134012.37	#Record13	
	2	Near	158690.158	#Records5	1.322
		Far	119991.66	#Record13	
	3	Near	141820.68	#Records5	1.328
		Far	106734.41	#Record13	
	4	Near	125671.188	#Records5	1.332
		Far	94277.84	#Record13	
	5	Near	110374.086	#Records5	1.334
		Far	82682.23	#Record13	
	6	Near	96007.611	#Records5	1.337
		Far	71795.98	#Record13	
	7	Near	82719.533	#Records5	1.343
		Far	61547.56	#Record13	
	8	Near	70536.314	#Records5	1.355
		Far	52049.92	#Record13	
	9	Near	59358.197	#Records5	1.331
		Far	44592.80	#Record13	
	10	Near	49175.739	#Records5	1.315
		Far	37395.97	#Record13	
	11	Near	40072.416	#Records5	1.309
		Far	30598.87	#Record13	
	12	Near	32366.182	#Records5	1.331
		Far	24306.65	#Record13	
	13	Near	25906.607	#Records5	1.393
		Far	18592.41	#Record13	
	14	Near	20058.394	#Records5	1.471
		Far	13630.37	#Record13	
	15	Near	14676.233	#Records5	1.542
		Far	9515.60	#Record13	
	16	Near	9936.677	#Records5	1.595
		Far	6228.99	#Record13	
	17	Near	6069.935	#Records5	1.628
		Far	3727.37	#Record13	
	18	Near	3293.378	#Records5	1.668
		Far	1973.30	#Record13	
	19	Near	1371.00	#Records5	1.690
		Far	811.22	#Record13	
	20	Near	409.456	#Records5	1.866
		Far	219.42	#Record13	

Table 8: Comparison of beam moment in 3-, 5-, 8-, and 20-story buildings subjected to near- and far-field earthquakes.

	Story	NF	Loc.	Record	FF	Loc.	Record	NF/FF
Beam moment (kN·m)	3	5.088	B_{32}	#Record10	3.986	B35	#Record6	1.28
	5	6.789	B_{42}	#Record10	5.810	B45	#Record6	1.17
	8	12.390	B_{42}	#Record15	14.320	B45	#Record12	0.87
	20	1593.300	B_{52}	#Records5	1373.670	B55	#Record13	1.16

near-field earthquake is greater than the amount if that under the effect of the far-field earthquake.

(ii) By investigating the structures analysis results, it can be observed that the average value of the maximum axial force in the columns of 3-, 8-, and 20-story structures under the effect of the near-field earthquake is 5%, 4%, and 38% greater than their values under the effect of the far-field earthquake, respectively. However, this value for the 5-story structure is almost the same in both situations.

(iii) The ratios of the average value of the maximum moments in the columns subjected to near- and far-field earthquakes in 3-, 5-, 8-, and 20-story structures were 1.03, 0.98, 1.03, and 1.33 respectively.

(iv) Regarding the assessment of the generated shear force on the buildings, it would be valid to claim that

Table 9: Ratios of PFAv/PGAv for the near-field earthquakes.

Records no.	Records name	PFAv (m/s^2)				Ratio of PFAv/PGAv			
		3-storey	5-storey	8-storey	20-storey	3-storey	5-storey	8-storey	20-storey
#Record1	Erzican	0.248	0.129	0.638	4.262	1.060	0.552	2.727	18.212
#Record2	Imperial Valley-EC-country	0.360	0.154	1.328	4.584	1.476	0.630	5.441	18.788
#Record3	Imperial Valley-Meloland	0.147	0.192	1.346	4.867	0.592	0.775	5.427	19.625
#Record4	Kobe-KJMA	0.201	0.153	0.296	8.344	0.596	0.454	0.875	24.687
#Record5	Kobe-PortIsland	0.300	0.238	2.562	10.877	0.530	0.420	4.527	19.217
#Record6	Kobe-Takatori	0.326	0.134	1.244	5.081	1.147	0.472	4.381	17.891
#Record7	Northridge-Newhall-fire st	0.269	0.250	0.814	11.327	0.490	0.457	1.485	20.669
#Record8	Imperial-BrawleyAirport	0.254	0.151	0.931	2.801	1.662	0.987	6.095	18.332
#Record9	Loma-Prieta-Valley	0.684	0.448	1.911	6.362	1.727	1.133	4.830	16.077
#Record10	Northridge-Rinaldi	0.639	0.663	4.108	17.840	0.667	0.693	4.288	18.622
#Record11	Northridge-Sylmar	1.046	0.332	4.964	10.117	1.728	0.548	8.206	16.722
#Record12	Imperial ElCentro10	0.144	0.107	0.664	2.386	1.321	0.986	6.088	21.889
#Record13	Imperial HoltvillePost	0.459	0.215	2.759	4.399	1.795	0.839	10.778	17.183
#Record14	LomaPieta GiloryArrar2	0.208	0.159	1.232	5.052	0.706	0.540	4.176	17.125
#Record15	LomaPieta GiloryArrar3	0.457	0.433	4.494	5.463	1.340	1.271	13.179	16.021

Table 10: Ratios of PFAv/PGAv for the far-field earthquakes.

Records no.	Records name	PFA_v (m/s^2)				Ratio $PFAv/PGA_V$			
		3-storey	5-storey	8-storey	20-storey	3-storey	5-storey	8-storey	20-storey
#Record1	Imperial Valley-CalexicoFireStation	0.637	0.304	1.751	3.255	3.302	1.577	9.075	16.866
#Record2	KocaeliTurkey-Duzce	0.481	0.230	2.268	4.558	2.334	1.117	11.009	22.126
#Record3	Landers-NorthPalmSprings	0.188	0.255	2.874	2.327	1.694	2.297	25.888	20.963
#Record4	Landers-YermoFireStation	0.174	0.131	1.230	2.725	1.281	0.965	9.057	20.067
#Record5	Loma Prieta-CoyoteLakeDam	0.109	0.045	0.457	1.928	1.149	0.470	4.812	20.292
#Record6	SanFernando-LA	0.294	0.308	2.417	2.457	1.794	1.877	14.738	14.981
#Record7	DesertHotSpr	0.107	0.116	0.675	2.619	0.902	0.977	5.673	22.009
#Record8	Imperial Valley-Delta	0.305	0.667	1.555	2.554	2.145	4.696	10.952	17.989
#Record9	Imperial Valley-El Centro Array	0.219	0.236	2.421	2.544	1.530	1.652	16.932	17.791
#Record10	Kobe-Shin-Osaka	0.049	0.026	0.088	1.591	0.771	0.411	1.392	25.260
#Record11	SuperstitionHills	0.336	0.098	0.630	2.870	2.644	0.775	4.958	22.595
#Record12	Loma Prieta-GilroyArray3	0.668	0.676	6.556	5.463	1.955	1.979	19.191	15.993
#Record13	Chi Chi Chy101	0.233	0.148	1.388	3.567	1.414	0.896	8.410	21.617
#Record14	Duzce Bolu	0.363	0.413	2.440	3.706	1.817	2.064	12.202	18.529
#Record15	Northridge Hollywood	0.258	0.205	1.123	2.576	1.707	1.358	7.439	17.061

the average of maximum created shear force in all structures (3-, 5-, 8-, and 20-story) subjected to the near-field earthquake was higher than the far-field one with the results of 10%, 5%, 14%, and 38%, respectively.

Data Availability

No data were used to support this study.

Conflicts of Interest

The authors declare that they have no conflicts of interest regarding the publication of this paper.

Acknowledgments

This research was supported by Basic Science Research Program through the National Research Foundation of Korea (NRF) funded by the Ministry of Science, ICT & Future Planning (2017R1A2B2010120).

References

[1] M. Dicleli and S. Buddaram, "Equivalent linear analysis of seismic-isolated bridges subjected to near-fault ground motions with forward rupture directivity effect," *Engineering Structures*, vol. 29, no. 1, pp. 21–32, 2007.

[2] B. Asgarian, A. Norouzi, P. Alanjari, and M. Mirtaheri, "Evaluation of seismic performance of moment resisting frames considering vertical component of ground motion," *Advances in Structural Engineering*, vol. 15, no. 8, pp. 1439–1453, 2012.

[3] S. Shahbazi, I. Mansouri, J. W. Hu, and A. Karami, "Effect of soil classification on seismic behavior of SMFs considering soil-structure interaction and near-field earthquakes," *Shock and Vibration*, vol. 2018, Article ID 4193469, 17 pages, 2018.

[4] S. Shahbazi, M. Khatibinia, I. Mansouri, and J. W. Hu, "Seismic evaluation of special steel moment frames undergoing near-field earthquakes with forward directivity by considering soil-structure interaction effects," *Scientia Iranica*, 2018, In press.

[5] Y. Bozorgnia, M. Niazi, and K. W. Campbell, "Characteristics of free-field vertical ground motion during the Northridge earthquake," *Earthquake Spectra*, vol. 11, no. 4, pp. 515–525, 1995.

[6] K. W. Campbell, "Empirical near-source attenuation relationships for horizontal and vertical components of peak ground acceleration, peak ground velocity, and pseudo-absolute acceleration response spectra," *Seismological Research Letters*, vol. 68, no. 1, pp. 154–179, 1997.

[7] M. Niazi and Y. Bozorgnia, "Behavior of near-source peak horizontal and vertical ground motions over SMART-1 array, Taiwan," *Bulletin-Seismological Society of America*, vol. 81, no. 3, pp. 715–732, 1991.

[8] M. Niazi and Y. Bozorgnia, "Behaviour of near-source vertical and horizontal response spectra at smart-1 array, Taiwan," *Earthquake Engineering & Structural Dynamics*, vol. 21, no. 1, pp. 37–50, 1992.

[9] W. Silva, "Characteristics of vertical strong ground motions for applications to engineering design," in *Proceedings of FHWA/NCEER Workshop on the National Representation of Seismic Ground Motion for New and Existing Highway Facilities*, Tech. Rep. No. NCEER-97-0010, pp. 205-252, Burlingame, CA, USA, May 1997.

[10] Y. Bozorgnia and K. W. Campbell, "Vertical ground motion model for PGA, PGV, and linear response spectra using the NGA-West2 database," *Earthquake Spectra*, vol. 32, no. 2, pp. 979–1004, 2016.

[11] Y. Bozorgnia and K. W. Campbell, "The vertical-to-horizontal response spectral ratio and tentative procedures for developing simplified V/H and vertical design spectra," *Journal of Earthquake Engineering*, vol. 8, no. 2, pp. 175–207, 2004.

[12] Z. Gülerce and N. A. Abrahamson, "Vector-valued probabilistic seismic hazard assessment for the effects of vertical ground motions on the seismic response of highway bridges," *Earthquake Spectra*, vol. 26, no. 4, pp. 999–1016, 2010.

[13] Z. Gülerce, R. Kamai, N. A. Abrahamson, and W. J. Silva, "Ground motion prediction equations for the vertical ground motion component based on the NGA-W2 database," *Earthquake Spectra*, vol. 33, no. 2, pp. 499–528, 2017.

[14] S. K. Kunnath, E. Erduran, Y. H. Chai, and M. Yashinsky, "Effect of near-fault vertical ground motions on seismic response of highway overcrossings," *Journal of Bridge Engineering*, vol. 13, no. 3, pp. 282–290, 2008.

[15] Y. Ohtori, R. E. Christenson, B. F. Spencer Jr., and S. J. Dyke, "Benchmark control problems for seismically excited nonlinear buildings," *Journal of Engineering Mechanics*, vol. 130, no. 4, pp. 366–385, 2004.

[16] HAZUS-MH MR5, *Multi-Hazard Loss Estimation Methodology: Earthquake Model*, Federal Emergency Management Agency, Washington, DC, USA, 2011.

[17] BHRC, *Iranian Code of Practice for Seismic Resistant Design of Buildings: Standard 2800*, BHRC, Tehran, Iran, 4th edition, 2014.

[18] M. R. Etemadi Mashhadi, "Development of fragility curves for seismic assessment of steel structures with consideration of soil-structure interaction," M.Sc. thesis, University of Brjand, Birjand, Iran, 2015, in Persian.

[19] OpenSees, *Open System for Earthquake Engineering Simulation*, PEER, 2018, http://opensees.berkeley.edu.

[20] A. Gupta and H. Krawinkler, "Seismic demands for performance evaluation of steel moment resisting frame structures," Technical Report 132, The John A. Blume Earthquake Engineering Research Center, Stanford University, Stanford, CA, USA, 1999.

[21] I. Mansouri and H. Saffari, "A new steel panel zone model including axial force for thin to thick column flanges," *Steel and Composite Structures*, vol. 16, no. 4, pp. 417–436, 2014.

[22] D. G. Lignos and H. Krawinkler, "Sidesway collapse of deteriorating structural systems under seismic excitations," Technical Report 172, The John A. Blume Earthquake Engineering Research Center, Stanford University, Stanford, CA, USA, 2009.

[23] L. F. Ibarra and H. Krawinkler, "Global collapse of frame structures under seismic excitations," Technical Report 152, The John A. Blume Earthquake Engineering Research Center, Ed., Stanford University, Stanford, CA, USA, 2005.

[24] S. L. Wu, B. Charatpangoon, J. Kiyono, Y. Maeda, T. Nakatani, and S. Y. Li, "Synthesis of near-fault ground motion using a hybrid method of stochastic and theoretical green's functions," *Frontiers in Built Environment*, vol. 2, pp. 1–16, 2016.

[25] L. Decanini, F. Mollaioli, and R. Saragoni, "Energy and displacement demands imposed by near-source ground motions," in *Proceedings of the 12th World Conference on Earthquake Engineering*, Auckland, New Zealand, January 2000.

[26] N. Gremer, C. Adam, R. A. Medina, and L. Moschen, "Vertical peak floor accelerations of elastic moment-resisting steel frames," *Bulletin of Earthquake Engineering*, pp. 1–22, 2019, In press.

[27] L. Moschen, R. A. Medina, and C. Adam, "Vertical acceleration demands on column lines of steel moment-resisting frames," *Earthquake Engineering & Structural Dynamics*, vol. 45, no. 12, pp. 2039–2060, 2016.